

Simulation of high angle annular dark field scanning transmission electron microscopy images of large nanostructures

J. Pizarro,^{1,a)} P. L. Galindo,¹ E. Guerrero,¹ A. Yáñez,¹ M. P. Guerrero,¹ A. Rosenauer,² D. L. Sales,³ and S. I. Molina³

¹Departamento de Lenguajes y Sistemas Informáticos, CASEM, Universidad de Cádiz, Campus Río San Pedro, s/n, 11510 Puerto Real, Cádiz, Spain

²Institute of Solid State Physics, University of Bremen, P.O. Box 330440, Bremen 28334, Germany

³Departamento de Ciencia de los Materiales e I. M. y Q. I., Facultad de Ciencias, Universidad de Cádiz, Campus Río San Pedro, s/n, 11510 Puerto Real, Cádiz, Spain

(Received 24 July 2008; accepted 22 September 2008; published online 14 October 2008)

High angle annular dark field scanning transmission electron microscopy (HAADF-STEM) is a powerful tool to quantify size, shape, position, and composition of nano-objects with the assessment of image simulation. Due to the high computational requirements needed, nowadays it can only be applied to a few unit cells in standard computers. To overpass this limitation, a parallel software (SICSTEM) has been developed. This software can afford HAADF-STEM image simulations of nanostructures composed of several hundred thousand atoms in manageable time. The usefulness of this tool is exemplified by simulating a HAADF-STEM image of an InAs nanowire. © 2008 American Institute of Physics. [DOI: 10.1063/1.2998656]

High angle annular dark field scanning transmission electron microscopy (HAADF-STEM), also known as Z-contrast,¹ is a technique that has demonstrated remarkable results for analyzing the composition and structure of nano-objects, reaching sub-Å resolution in aberration-corrected microscopes. Nevertheless, simulations are limited to objects composed of a few unit cells in standard computers. This paper introduces a parallel HAADF-STEM simulation software (SICSTEM), capable of simulating images from large nanostructures in reasonable time (from hours to a few days).

When an electron wave propagates through a crystal, the wave function at its exit surface can be calculated by the multislice algorithm.² In this method the crystal is divided into thin slices and the wave function ψ after the n th slice is given by

$$\Psi_n(x) = [q_n(x)\Psi_{n-1}(x)] \otimes pn(x), \quad (1)$$

where q_n and p_n are the transmission function (the phase grating) and the propagator function for the n th slice, respectively, the symbol \otimes represents the convolution operation and the vector x indicates a two-dimensional position over the slice. Quantitative analysis of HAADF-STEM imaging requires the simulation of elastic scattering³ and incoherent thermal diffuse scattering⁴ (TDS). The interest in TDS is growing because HAADF contrast is mostly determined by TDS.⁵ While the frozen phonon method approaches the exact image intensity if a large number of configurations is used,^{5,6} this method is very time consuming and a number of alternatives have been developed to include TDS in calculation of the intensity in the object exit plane by the multislice method using a local TDS absorptive potential approach.⁷⁻¹³ In this software, TDS intensity calculations are based on the STEM-SIM program,¹⁴ according to Refs. 7 and 10. This approach is an approximation in good agreement with the frozen lattice method at small specimen thicknesses, typically below 50 nm.¹⁵

^{a)}Electronic mail: joaquin.pizarro@uca.es.

Let ψ_{incident} be an incident wave described as $\psi_{\text{incident}} = \sum_g \psi_g \exp(2\pi i \mathbf{g} \cdot \mathbf{r})$, the probability for scattering of the incident wave with scattering vector S due to a thermally displaced atom n is given by

$$\begin{aligned} P_S^n &= \langle \exp(2\pi i \mathbf{S} \cdot \mathbf{r}) | V_n(\mathbf{r} - \mathbf{r}_n - \mathbf{u}_n) | \sum_g \Psi_g \exp(2\pi i \mathbf{g} \cdot \mathbf{r}) \rangle \\ &= \sum_g \Psi_g \exp[-2\pi i (\mathbf{S} - \mathbf{g}) \cdot (\mathbf{r}_n + \mathbf{u}_n)] \\ &\quad \times \int V_n(\mathbf{r}) \exp[-2\pi i (\mathbf{S} - \mathbf{g}) \cdot \mathbf{r}] d^3\mathbf{r} \\ &= \sum_g \Psi_g \exp[-2\pi i (\mathbf{S} - \mathbf{g}) \cdot (\mathbf{r}_n + \mathbf{u}_n)] f_{S-g}^n, \end{aligned} \quad (2)$$

where V_n is the Coulomb potential of atom n , r is a vector in real space, and r_n and u_n are the equilibrium position and displacement of atom n , respectively. Then, the intensity on the detector stemming from a certain slice is computed by

$$\begin{aligned} I_{\text{detector}} &= C \int_{\text{detector}} \langle | \sum_{\text{atoms in slice } n} P_S^n |^2 \rangle_{\text{time average over } U_n} \\ &\quad \times dS = I_{\text{Bragg}} + I_{\text{TDS}} \\ I_{\text{TDS}} &= C \sum_g \sum_h \Psi_g \Psi_h^* \left\{ \sum_n \exp[2\pi i (\mathbf{g} \right. \\ &\quad \left. - \mathbf{h}) \cdot \mathbf{r}_n] \int_{\text{detector}} f_{S-g}^n f_{S-g}^{*n} E d\mathbf{S} \right\} \\ &= C \sum_g \sum_h \Psi_g \Psi_h^* V_{h,g}, \end{aligned} \quad (3)$$

where $C = \sigma^2 \Delta z / \Omega$ and $E = \exp[-M_n(\mathbf{g} - \mathbf{h})^2] - \exp[-M_n(\mathbf{S} - \mathbf{g})^2 - M_n(\mathbf{S} - \mathbf{h})^2]$, Ω is the volume of crystal cell, $\sigma = 2\pi m_0 e \lambda / h^2$ and M_n is the Debye-Waller temperature factor of atom n , related with the mean square atomic displacement by $M = 2\pi^2 \langle u^2 \rangle$.

Using the local approximation $V_{\mathbf{h},\mathbf{g}}^{\text{HAADF}} \approx V_{\mathbf{h}-\mathbf{g},0}^{\text{HAADF}}$ we obtain

$$I_{\text{TDS}} = C \sum_g \sum_h \Psi_g \Psi_h^* V_{\mathbf{h}-\mathbf{g}}^{\text{HAADF}} \quad (4)$$

and applying the inverse Fourier transform $V^{\text{HAADF}}(\mathbf{R}) = FT_{\mathbf{h}-\mathbf{g} \rightarrow \mathbf{R}}\{V_{\mathbf{h}-\mathbf{g}}^{\text{HAADF}}\}$ we get

$$\begin{aligned} I_{\text{TDS}} &= C \sum_g \sum_h \Psi_g \Psi_h^* \left\{ \int V^{\text{HAADF}}(\mathbf{R}) \exp(2\pi i(\mathbf{g} - \mathbf{h}) \cdot \mathbf{R}) d^2\mathbf{R} \right\} = C \int V^{\text{HAADF}}(\mathbf{R}) \\ &\times \left\{ \sum_g \sum_h \Psi_g \Psi_h^* \exp(2\pi i(\mathbf{g} - \mathbf{h}) \cdot \mathbf{R}) d^2\mathbf{R} \right\} \\ &= C \int V^{\text{HAADF}}(\mathbf{R}) \\ &\times \left\{ \sum_g \Psi_g \exp(2\pi i\mathbf{g} \cdot \mathbf{R}) \sum_h \Psi_h^* \exp(2\pi i\mathbf{h} \cdot \mathbf{R}) \right\} \\ &\times d^2\mathbf{R} = C \int V^{\text{HAADF}}(\mathbf{R}) \{\Psi(\mathbf{R})\Psi^*(\mathbf{R})\} d^2\mathbf{R} \\ &= C \int V^{\text{HAADF}}(\mathbf{R}) I_{\text{Bragg}}(\mathbf{R}) d^2\mathbf{R}. \quad (5) \end{aligned}$$

Finally, the total TDS intensity on the detector is computed by summing up contributions from all slices and adding the Bragg scattered elastic intensity. Nevertheless this approach is still computationally intensive for large supercells. In order to cope with this problem, a parallel code named SICSTEM has been developed on the basis of the STEM-SIM (Ref. 14) program.

The input to SICSTEM software is a supercell (described as a set of $\langle x, y, z \rangle$ coordinates for atom positioning, its composition, site occupancy, and Debye–Waller factor) and the characteristics of the microscope (beam energy, third and fifth order objective aberrations, objective aperture, detector angles, etc.). The atoms are sorted by depth (along z) and then sliced into layers of a specified thickness. The software calculates the projected atomic potential for each slice taking into account the TDS. This step can be easily made in parallel because potentials are independent to each other. However, the most demanding routine is the multislice simulation. At each desired position of the specimen, an incident focused probe wave function is generated, and then transmitted and propagated across the specimen taking into account phase grating and TDS until it reaches the exit surface. Finally, the electron intensity is integrated on the detector. In HAADF-STEM simulation, the calculation of each pixel requires a complete multislice simulation (thus requiring more than 1×10^6 multislice calculations for a 1024×1024 image). Nevertheless, each pixel in the scanning process can be calculated independently from each other, making easy the division of tasks in parallel. The software has been designed to be able to generate not only one-dimensional line scans or two-dimensional images, but also focal series, very useful in three-dimensional (3D) HAADF-STEM research.

In order to test the accuracy of the software, two different simulation results are shown for small cells. A line profile of STEM-HAADF image of pure InAs has been compared

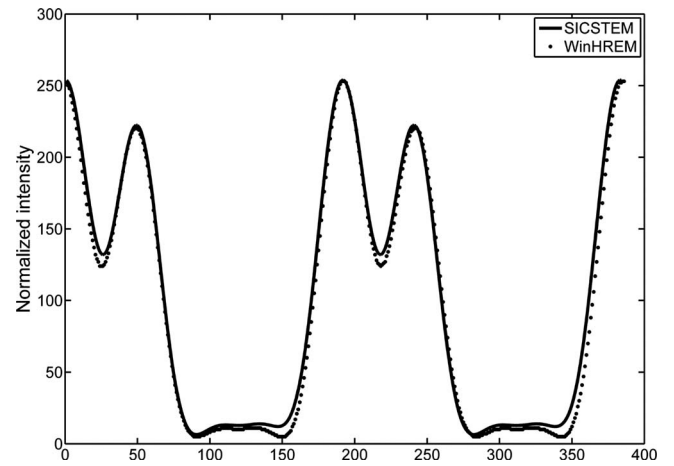


FIG. 1. Comparison of STEM-HAADF simulated line profiles of pure InAs generated using SICSTEM code and STEM extension to WINHREM software.

(Fig. 1) with that obtained using STEM for WinHREM™ (HREM Research Inc., Japan) for the same imaging conditions and displacement parameters. In order to test the accuracy across variations in thickness, the contrast ratio of Ga/As peaks has been determined for thickness values in the range of 0–20 nm. The displacement parameter used for Ga and As were 0.687 and 0.568 Å², respectively. Figure 2 illustrates a comparison with Ishizuka's Fast Fourier Transform (FFT) multislice approach,⁶ where the contrast ratio of As/Ga peaks as a function of specimen thickness is shown.

We have run the software in order to get a HAADF-STEM simulated image of an InP capped InAs_xP_{1-x}/InP nanowire. The composition assumed for the test nanowire is taken from a previous publication,¹⁶ assuming that the maximum composition in the nanowire is 100% (pure InAs). The nanowire is oriented along $[1\bar{1}0]$ and periodically arranged along $[110]$. The electron beam propagates along $[1\bar{1}0]$. The image was simulated considering a 100 kV dedicated VG

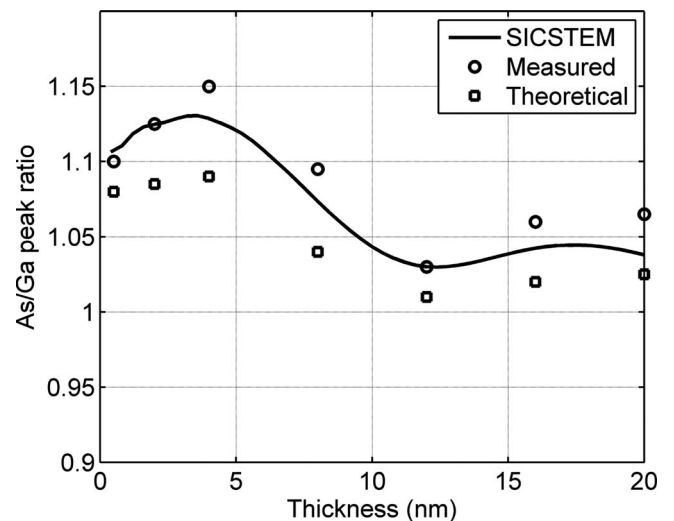


FIG. 2. Contrast ratio of As/Ga peaks as a function of specimen thickness. Dots and squares represent the contrast ratios calculated using Ishizuka's FFT multislice code for the measured displacement values (0.687 and 0.568 Å² for Ga and As, respectively) and for the theoretical estimates (0.637 and 0.685 Å² for Ga and As, respectively) (Ref. 6). The line represents the As/Ga peak ratio obtained by SICSTEM software using displacement values (0.687 and 0.568 Å²).

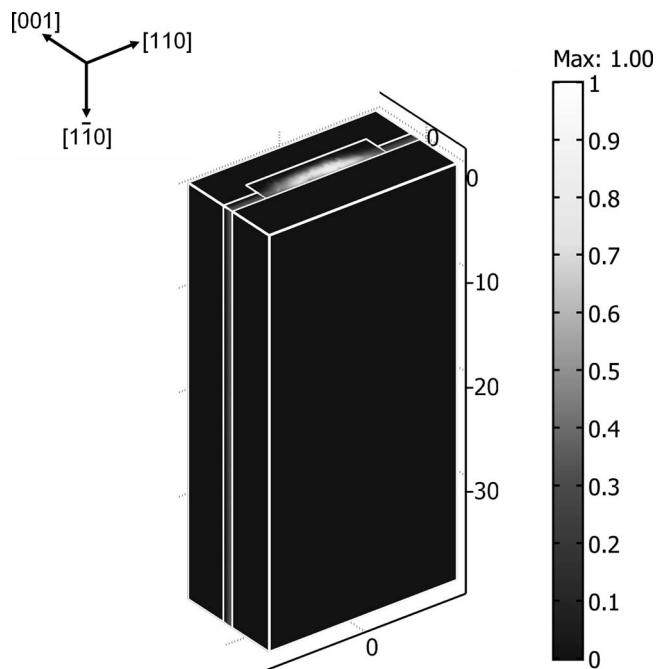


FIG. 3. 3D model ($20 \times 10 \times 40 \text{ nm}^3$) representing As concentration in the $\text{InAs}_x\text{P}_{1-x}$ nanowire used as input to the SICSTEM image simulation software.

Microscope HB501UX STEM, $C_s = -50 \mu\text{m}$, $C_5 = 63 \text{ mm}$, inner detector angle = 70 mrad , outer detector angle = 200 mrad , and objective aperture = 27 mrad , which gives a probe size of $\sim 0.85 \text{ \AA}$. A commercial finite element analysis (FEA) package has been used to describe the geometry of the nanostructure (subdomains, boundaries, constraints, symmetries, etc.) and to define the local parameters (composition, initial strains, elastic constants, etc.). It is assumed that As composition along z (coordinate along 001) remains constant. The capping layer and substrate were assumed to be pure InP. Model size was defined to be $20 \times 10 \times 40 \text{ nm}^3$. Figure 3 shows the compositional map and model used in the simulation. The periodicity of the structure was chosen to be 20 nm and it was taken into account by applying the appropriate boundary conditions. A supercell was created by replicating the substrate unit cell coordinates across three dimensions of space. To take into account surface relaxation effects the displacement field was obtained from the model by solving the equations of the anisotropic elastic theory and modifying supercell atom properties (i.e., atom coordinates, occupancy, and Debye–Waller factors) using imported values from the FEA model at equilibrium. This approach has been applied to predict the preferential nucleation sites in InAs self-assembled nanowires^{17,18} and to determine the strain fields in nano-objects.^{19,20} The number of atoms in the supercell was 422 184. The supercell was sliced into 68 layers of $5.8687 \text{ \AA}/\text{layer}$. The simulated image of the nanowire is shown in Fig. 4. This image has been obtained at the supercomputer of the University of Cadiz, a cluster composed of 80 nodes, each consisting of two Intel Dual Core Xeon 5160 and 8 MB of random access memory, being the overall number of cores equal to $80 \times 2 \times 2 = 320$ and achieving a peak performance of 3.75 TFLOPS (1 TFLOP = 10^{12} floating point operations per second). The processing time was 78 h for a 560×1024 pixels resolution image.

In summary, a software code for the simulation of HAADF-STEM images of large supercells has been devel-

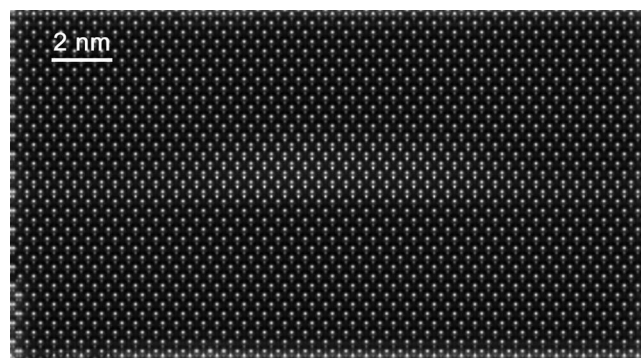


FIG. 4. HAADF-STEM image of an $\text{InAs}_x\text{P}_{1-x}$ nanowire (560×1024 pixels) simulated using SICSTEM.

oped and its accuracy has been compared to Ishizuka's FFT multislice approach and to STEM for WinHREM™ software. A methodology has been set up to simulate HAADF-STEM images of large nanostructures, and its usefulness has been demonstrated for an $\text{InAs}_x\text{P}_{1-x}/\text{InP}$ nanowire represented by a supercell of nearly half a million atoms.

This work was supported by the SANDiE European Network of Excellence (Contract No NMP4-CT-2004–500101), the Spanish MEC (Contract Nos. TEC2005–05781-C03–02 and MAT2007–60643), and the Junta de Andalucía (PAI Research Groups TEP-120 and TIC-145 Project No. PAI05-TEP-00383).

- ¹S. J. Pennycook, B. Rafferty, and P. D. Nellist, *Microsc. Microanal.* **6**, 343 (2000).
- ²J. M. Cowley and A. F. Moodie, *Acta Crystallogr.* **10**, 609 (1957).
- ³P. D. Nellist and S. J. Pennycook, *Ultramicroscopy* **78**, 111 (1999).
- ⁴P. Xu, R. F. Loane, and J. Silcox, *Ultramicroscopy* **38**, 127 (1991).
- ⁵Z. L. Wang, *Acta Crystallogr., Sect. A: Found. Crystallogr.* **51**, 569 (1995).
- ⁶E. J. Kirkland, *Advanced Computing in Electron Microscopy* (Plenum, New York, 1998).
- ⁷K. Ishizuka, *Ultramicroscopy* **90**, 71 (2002).
- ⁸K. Watanabe, T. Yamazaki, I. Hashimoto, and M. Shiojiri, *Phys. Rev. B* **64**, 115432 (2001).
- ⁹C. J. Rossouw, L. J. Allen, S. D. Findlay, and M. P. Oxley, *Ultramicroscopy* **96**, 299 (2003).
- ¹⁰S. D. Findlay, L. J. Allen, M. P. Oxley, and C. J. Rossouw, *Ultramicroscopy* **96**, 65 (2003).
- ¹¹S. J. Pennycook and D. E. Jesson, *Phys. Rev. Lett.* **64**, 938 (1990).
- ¹²S. J. Pennycook and D. E. Jesson, *Ultramicroscopy* **37**, 14 (1991).
- ¹³C. R. Hall and P. B. Hirsch, *Proc. R. Soc. London, Ser. A* **286**, 158 (1965).
- ¹⁴A. Rosenauer and M. Schowalter, *Springer Proceedings in Physics: Microscopy of Semiconducting Materials 2007* (Springer, New York, 2007), Vol. 120, p. 169.
- ¹⁵J. M. LeBeau, S. D. Findlay, L. J. Allen, and S. Stemmer, *Phys. Rev. Lett.* **100**, 206101 (2008).
- ¹⁶S. I. Molina, M. Varela, T. Ben, D. Sales, J. Pizarro, P. Galindo, D. Fuster, Y. González, L. González, and S. Pennycook, *J. Nanosci. Nanotechnol.* **8**, 3422 (2008).
- ¹⁷S. I. Molina, T. Ben, D. L. Sales, J. Pizarro, P. L. Galindo, M. Varela, S. J. Pennycook, D. Fuster, Y. Gonzalez, and L. Gonzalez, *Appl. Phys. Lett.* **91**, 143112 (2007).
- ¹⁸S. I. Molina, T. Ben, D. L. Sales, J. Pizarro, P. L. Galindo, M. Varela, S. J. Pennycook, D. Fuster, Y. Gonzalez, and L. Gonzalez, *Nanotechnology* **17**, 5652 (2006).
- ¹⁹S. I. Molina, M. Varela, D. L. Sales, T. Ben, J. Pizarro, P. L. Galindo, D. Fuster, Y. González, L. González, and S. J. Pennycook, *Microsc. Microanal.* **13**, Suppl. s02, 146 (2007).
- ²⁰D. L. Sales, J. Pizarro, P. L. Galindo, R. García, G. Trevisi, P. Frigeri, L. Nasi, S. Franchi, and S. I. Molina, *Nanotechnology* **18**, 475503 (2007).